Hydrodynamical simulations of a compact source scenario for G2

A. Ballone[1,2], M. Schartmann[1,2], A. Burkert[1,2,3], S. Gillessen[2], R. Genzel[2], T. K. Fritz[2], F. Eisenhauer[2], O. Pfuhl[2] and T. Ott[2]

[1]University Observatory Munich, Scheinerstraße 1, D-81679 München, Germany
email: `aballone@mpe.mpg.de`

[2]Max-Planck-Institute for Extraterrestrial Physics, Postfach 1312, Giessenbachstraße, D-85741 Garching, Germany

[3]Max-Planck Fellow

Abstract. The origin of the dense gas cloud "G2" discovered in the Galactic center (Gillessen *et al.* 2012) is still a debated puzzle. G2 might be a diffuse cloud or the result of an outflow from an invisible star embedded in it. We present here detailed simulations of the evolution of winds on G2's orbit. We find that the hydrodynamic interaction with the hot atmosphere present in the Galactic center and the extreme gravitational field of the supermassive black hole must be taken into account when modeling such a source scenario. We also find that in this scenario most of the Brγ luminosity is expected to come from the highly filamentary densest shocked wind material. G2's observational properties can be used to constrain the properties of the outflow and our best model has a mass outflow rate of $\dot{M}_\mathrm{w} = 8.8 \times 10^{-8}\mathrm{M}_\odot\mathrm{yr}^{-1}$ and a wind velocity of $v_\mathrm{w} = 50\mathrm{km\,s}^{-1}$. These values are compatible with those of a young TTauri star wind, as already suggested by Scoville & Burkert (2013).

Keywords. Galaxy: center, individual (Sgr A*, G2) — methods: numerical

1. Introduction

In the last year, the discovery of the object G2 in our Galactic center (Gillessen *et al.* 2012, 2013a,b) has caught the attention of the astronomical community. The object has been detected in the *L*-band with the infrared imager NACO and with the integral field spectrograph SINFONI at the VLT in Brackett-γ, He I and Paschen-α line emission. The detection in these bands has also been confirmed by Eckart *et al.* (2013) and Phifer *et al.* (2013), even if the nature of this object is still controversial. With the help of observations from the last 10 yr, Gillessen *et al.* (2012) and Gillessen *et al.* (2013a,b) derived the dynamical properties of the object, finding that G2 is orbiting around the supermassive black hole on a very eccentric orbit ($e \approx 0.98$), with pericenter at 2400 Schwarzschild radii, which G2 is expected to reach in early 2014.

There are two main scenarios for the nature of G2. The first one is the so-called *diffuse cloud scenario* for which G2 is a dense and compact clump: in this case the *L*-band emitting material is a warm dust component with temperature $T_\mathrm{dust} \approx 550\mathrm{K}$, while the line emission comes from an ionized gas ($T_\mathrm{gas} \approx 10^4\mathrm{K}$) component, with roughly constant Brγ luminosity $L_\mathrm{Br\gamma} \approx 2 \times 10^{-3}\mathrm{L}_\odot$ between 2004 and 2013. Gillessen *et al.* (2012) have derived, from the observed size and Brγ luminosity, a density of about $\rho_\mathrm{c} \approx 6.1 \times 10^{-19}\mathrm{gcm}^{-3}$, with a corresponding mass of $M_\mathrm{G2} \approx 1.7 \times 10^{28}\mathrm{g} \approx 3$ Earth masses. Interestingly, the observed orbit of G2 roughly lies in the plane of the clockwise rotating disk of young and massive stars ranging from 0.04pc to 0.5pc around the central hot bubble (Genzel *et al.* 2003, Paumard *et al.* 2006, Alig *et al.* 2013), so G2 could

be a compact gas cloud that formed as a result of stellar wind interactions (Cuadra *et al.* 2006, Gillessen *et al.* 2012, Burkert *et al.* 2012). Burkert *et al.* (2012), Schartmann *et al.* (2012) and Anninos *et al.* (2012) study in high detail the evolution and fate of such an object with the properties of G2.

The second scenario for G2 is the so-called *compact source scenario*, for which G2 is the outflow from a star in its center. Murray-Clay & Loeb (2012) show that the observed properties of G2 can be explained by gas outflowing from a photoevaporating protoplanetary disk and being tidally stripped while reaching Sgr A* (a similar scenario has also been proposed by Miralda-Escudé 2012). Meyer & Meyer-Hofmeister (2012) investigate the possibility that a nova, being on a similar orbit, could produce an expanding shell, while Scoville & Burkert (2013) suggest that the observed emission could come from the tip of an inner, thin and *cold bow shock*, produced by the wind of a TTauri star plunging into Sgr A*.

The *compact source scenario* has been studied up to now only with simplified analytic approximations. The aim of our work is to study these effects for a large range of outflow parameters with the help of hydrodynamic simulations with the Eulerian code PLUTO (Mignone *et al.* 2012).

2. Simulations setup

To simplify our model, we simulated a single spherical wind moving in a two dimensional uniform grid in cylindrical coordinates (Z, R), This led us to simplify our problem, assuming a zero angular momentum orbit. This is not a severe restriction when the source is far enough from pericenter, since the observed orbit has a very high eccentricity $e \simeq 0.98$ (Gillessen *et al.* 2013b). We simulated almost the entire domain of the orbit from G2's apocenter, at $Z = -1.64 \times 10^{17}$cm (from the orbital derivation of Gillessen *et al.* 2013a), to very close to Sgr A*, fixing the frame of reference on the SMBH. The wind outflows are modeled with a mechanical approach, i.e. fixing constant density and velocity in a very small circular input region, in order to reproduce the correct injection of mass on its outer boundary. The input region is following G2's observed orbit with time. An adiabatic index $\Gamma = 1$ is assumed. This choice is based on the assumption that the shocked wind is so dense and cools so fast that it can be treated as being isothermal (Scoville & Burkert, 2013). The hot atmosphere is modeled following the density and temperature distribution used by Schartmann *et al.* (2012), while the supermassive black hole's gravitational field is assumed to be a Newtonian point-source with mass $M_{\rm BH} = 4.31 \times 10^6 {\rm M}_\odot$ (Gillessen *et al.* 2009) at $Z, R = 0$.

We refer to Ballone *et al.* (2013) for more numerical details.

3. Results and discussion

Our standard and best model has $\dot{M}_{\rm w} = 8.8 \times 10^{-8} {\rm M}_\odot {\rm yr}^{-1}$ and $v_{\rm w} = 50 {\rm km \, s}^{-1}$. Figure 2 shows the evolution of the density with time (and with the motion towards the supermassive black hole). Our simulations show that the presence of a surrounding high-temperature atmosphere (like that predicted by ADAF/RIAF solutions for the diffuse X-ray emission in the Galactic center, e.g. Yuan *et al.* 2003) could be very important when modeling any *compact source scenario* for G2. Due to the high pressure of the atmosphere, the structure of the studied winds is very different from that of typical stellar winds. As already shown by Scoville & Burkert (2013), the free-streaming wind interacting with this hot atmosphere will be shocked and already at early stages a very thin, dense and Rayleigh-Taylor unstable shell of shocked wind material forms around
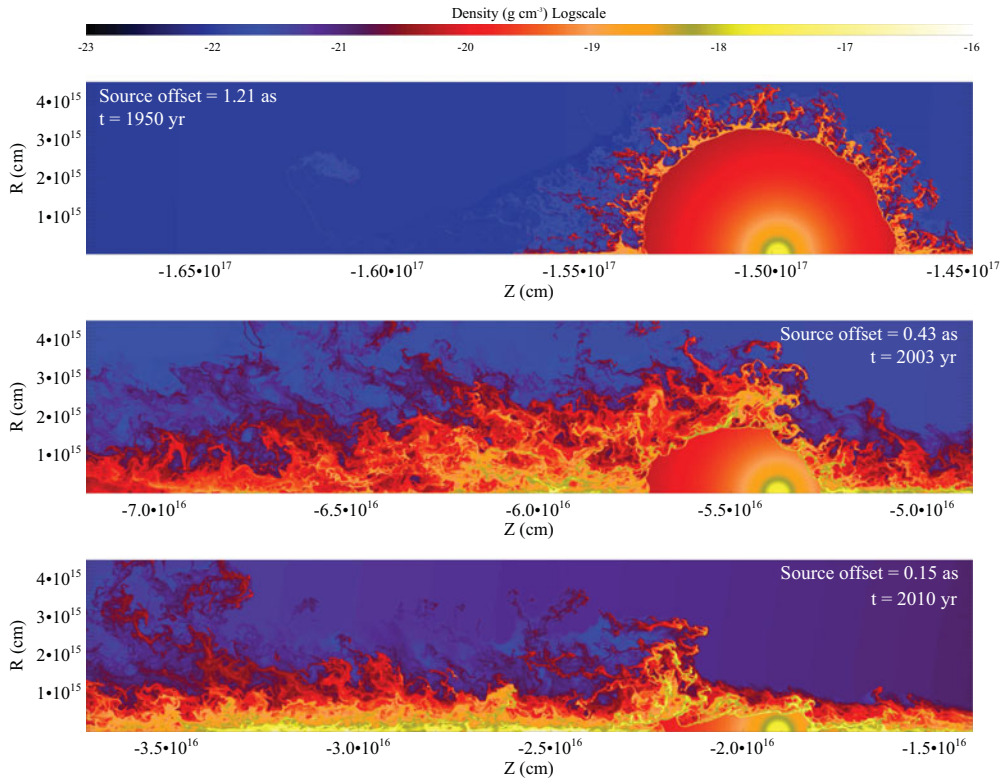
Figure 1. Density maps for our standard model, for source distances of $1.21''$, $0.43''$, and $0.15''$ from Sgr A* (from top to bottom). [A COLOR VERSION IS AVAILABLE ONLINE.]

the free wind region. This is, along with the $1/r^2$ density distribution of the free-wind region, the main difference with respect to the *diffuse cloud scenario*, where the object has instead a more or less uniform density all over its volume. Differently from the *diffuse cloud scenario*, at late phases the ram pressure of the atmosphere can have an important role in affecting the structure of the wind (via stripping of wind material), while, as in the *diffuse cloud scenario*, the dominant process at late phases is the squeezing and compression of the object in the direction perpendicular to the motion by the SMBH extreme tidal field. A simple coupling of all these different effects is hard to perform in an analytic study.

Figure 3 shows the evolution of the Brγ luminosity. Our calculation for the best model gives a luminosity which is comparable with the observed ones, even if it increases significantly toward pericenter, while the observed one has roughly a constant value. Interestingly, most of the luminosity in such a scenario comes from the filamentary densest shocked wind material, as visible in the lower panel of Figure 3. This is another main difference with the *diffuse cloud scenario*, where the emission is generated by diffuse gas with rather uniform density. Figure 3 also shows that the size of G2 in the position-velocity diagrams can also be reproduced by the standard model.

We have finally made a small wind parameters study to constrain the properties of the outflow. We have hence divided and multiplied the wind mass-loss rate and velocity by a factor of 5, respectively. Such a small factor already gives significant differences in the resulting observational properties (e.g., roughly a factor of 10 different luminosities). As summarized in Figure 3., when fixing the mass-loss rates, a higher velocity gives a
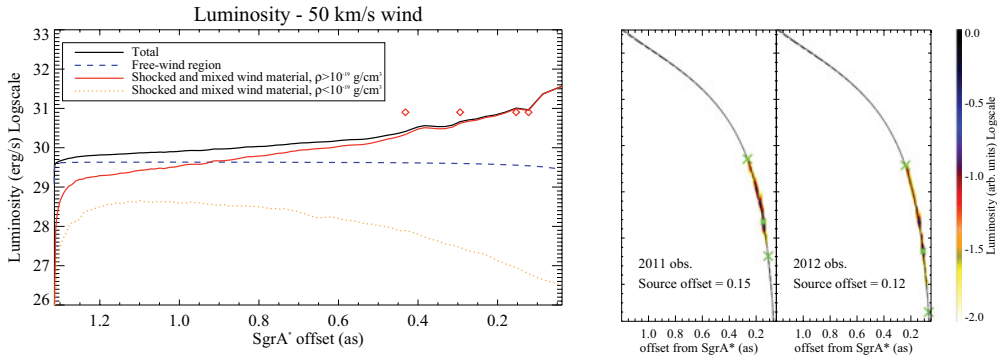
Figure 2. Left panel: Brγ luminosity evolution for our standard model. The solid line shows the total luminosity, the dashed line shows the luminosity of the free-wind region, the dash-dotted line shows the luminosity of the shocked wind with densities $> 10^{-19}$ gcm^{-3}, and the dotted line shows the luminosity of the shocked wind material with densities $< 10^{-19}$ gcm^{-3}. The red diamonds represent the observations. **Right:** position-velocity diagrams for our standard model, for a source distance of $0.15''$, and $0.12''$ from Sgr A*. The green crosses show the G2 observed extremes and the green asterisk shows the position of the source in the diagram. [A COLOR VERSION IS AVAILABLE ONLINE.]

	lower $\dot{M}_w$	$\dot{M}_w = 8.8 \times 10^{-8} \, M_\odot/yr$	higher $\dot{M}_w$
higher v_w	- possible observed size - lower luminosity	HV: - larger size - lower luminosity	- larger size - possible observed luminosity
$v_w = 50 \, km/s$	LMDOT: - smaller size - lower luminosity	standard model	HMDOT: - larger size - higher luminosity
lower v_w	- smaller size - possible observed luminosity	LV: - smaller size - higher luminosity	- possible observed size - higher luminosity

Figure 3. Dependence of G2 luminosity and size on the wind parameters.

lower luminosity and a larger size of the emitting material (and vice versa). At constant velocity, a higher mass loss rate is instead leading to a higher luminosity and a larger size (and vice versa). Thus, a combination of observed size and luminosity can effectively constrain the wind parameters. For our choice of the atmosphere, the wind parameters of our best model are comparable with those of a young TTauri star wind (White & Hillenbrand 2004). The age of TTauri stars is also consistent with the age ($\simeq 6 \pm 2$Myr, Paumard *et al.* 2006) of the clockwise disk of young stars, where the source could have been scattered from (Murray-Clay & Loeb 2012).

References

Alig, C., Schartmann, M., Burkert, A. & Dolag, K. 2013, *ApJ* 771, 119
Anninos, P., Fragile, P. C., Wilson, J. & Murray, S. D. 2012, *ApJ* 759, 132
Ballone, A., Schartmann, M., Burkert, A., Gillessen, S., Genzel, R. *et al.* 2013, *ApJ* 776, 13
Burkert, A., Schartmann, M., Alig, C., Gillessen, S., Genzel *et al.* 2012, *ApJ* 750, 58
Cuadra, J., Nayakshin, S., Springel, V. & Di Matteo, T. 2006, *MNRAS* 366, 358
Eckart, A., Mužić, K., Yazici, S., Sabha, N., Shahzamanian *et al.* 2013, *A&A* 551, A18
Genzel, R., Schödel, R., Ott, T., Eisenhauer, F., Hofmann, R. *et al.* 2003, *ApJ* 594, 812
Gillessen, S., Eisenhauer, F., Trippe, S., Alexander, T., Genzel, R. *et al.* 2009, *ApJ* 692, 1075
Gillessen, S., Genzel, R., Fritz, T. K., Quataert, E., Alig, C. *et al.* 2012, *Nature* 481, 51
Gillessen, S., Genzel, R., Fritz, T. K., Eisenhauer, F., Pfuhl, O. *et al.* 2013a, *ApJ* 763, 78
Gillessen, S., Genzel, R., Fritz, T. K., Eisenhauer, F., Pfuhl, O. *et al.* 2013b, *ApJ* 774, 44

Meyer, F., & Meyer-Hofmeister, E. 2012, *A&A* 546, L2

Mignone, A., Zanni, C., Tzeferacos, P., van Straalen, B., Colella, P. *et al.* 2012, *ApJS* 198, 7

Miralda-Escudé, J. 2012, *ApJ* 756, 86

Murray-Clay, R. A., & Loeb, A. 2012, *NatCo* 3, 1049

Paumard, T., Genzel, R., Martins, F., Nayakshin, S., Beloborodov *et al.* 2006, *ApJ* 594, 812

Phifer, K., Do, T., Meyer, L., Ghez, A. M., Witzel *et al.* 2013, *ApJL* 773, L13

Schartmann, M., Burkert, A., Alig, C., Gillessen, S., Genzel, R. *et al.* 2012, *ApJ* 750, 58

Scoville, N., & Burkert, A. 2013, *ApJ* 768, 108

White, R. J., & Hillenbrand, L. A. 2004, *ApJ* 616, 998

Yuan, F., Quataert, E. & Narayan, R. 2003, *ApJ* 598, 301